

Proton-proton and deuteron-gold collisions at RHIC

Klaus Werner^{(a)1}, Fuming Liu^(b,c), Tanguy Pierog^(d)

^(a) SUBATECH, Université de Nantes – IN2P3/CNRS – Ecole des Mines, Nantes, France

^(b) Institute of Particle Physics, Huazhong Normal University, Wuhan, China

^(c) Institut für Theoretische Physik, J. W. Goethe Universität, Robert-Mayer-Str. 10, 60054 Frankfurt am Main, Germany

^(d) FZK, Institut für Kernphysik, Karlsruhe, Germany

Abstract

We try to understand recent data on proton-proton and deuteron-gold collisions at RHIC, employing a modified parton model approach.

1 Interesting data from RHIC

The nuclear modification factor $R = (dN_{AA}/d^2p_t) / (N_{\text{coll}} dN_{pp}/d^2p_t)$ shows interesting features: For AuAu, it is much smaller than one for central collisions, whereas for d-Au, it is bigger than one for central collisions. With decreasing centrality, the modification factor for d-Au approaches one and goes even below one. Also interesting is the fact that R decreases with increasing pseudo-rapidity (see fig 1, data from [1, 2]).

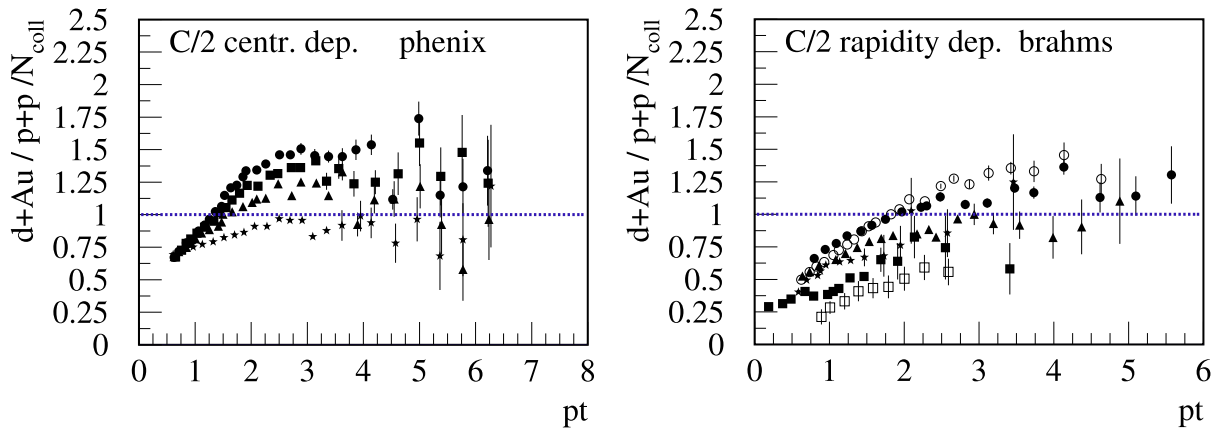


Figure 1: Left: Centrality dependence of the nuclear modification factor. Top to bottom: 0-20%, 20-40%, 40-60%, 60-88%. Right: Rapidity dependence of the nuclear modification factor. Top to bottom: $\eta = 0, 1, 2.2, 3.2$.

¹Invited talk, given at the XXth Winter Workshop on Nuclear Dynamics, Trelawny Beach, Jamaica, March 2004.

2 High parton densities

In this chapter we want to discuss theoretical implications of high parton densities.

Let us first consider parton-parton scattering. A parton from the projectile, after emitting several (initial state) partons, interacts with a corresponding parton from the target, see figure 2(left). To simplify further discussions, we use a symbolic parton ladder for this diagram, as shown in figure 2(right).

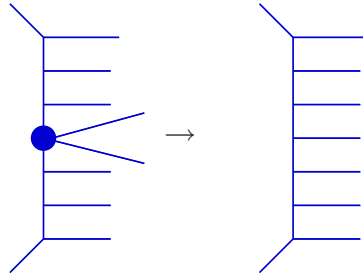


Figure 2: Parton-parton scattering.

Having several partons available, the projectile parton may interact in this way with any of the target partons, as shown in fig. 3, and vice versa, this will simply change the cross section by some factor.

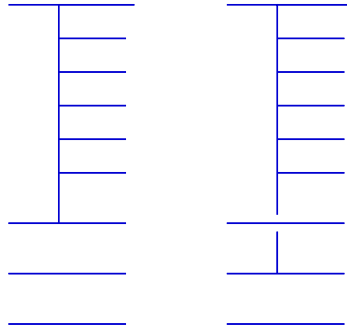


Figure 3: Scattering with many partons.

The situation will, however, be more complicated in case of high parton densities. Here, a parton from a ladder may rescatter with another target from the projectile or target, providing an additional ladder (fig. 4, left). A ladder parton may also interact elastically (fig. 4, middle). And finally, a parton ladder may be linked to two closed ladders (fig. 4, right), providing a rapidity gap on the projectile or target side. Diagram (B) will interfere with the simple diagram (fig. 3), and gives a negative contribution to the cross section, providing screening. Diagram (C) can be referred to as high mass diffraction. Particularly interesting is diagram (A), the case of multiple parton ladders, as we are going to discuss

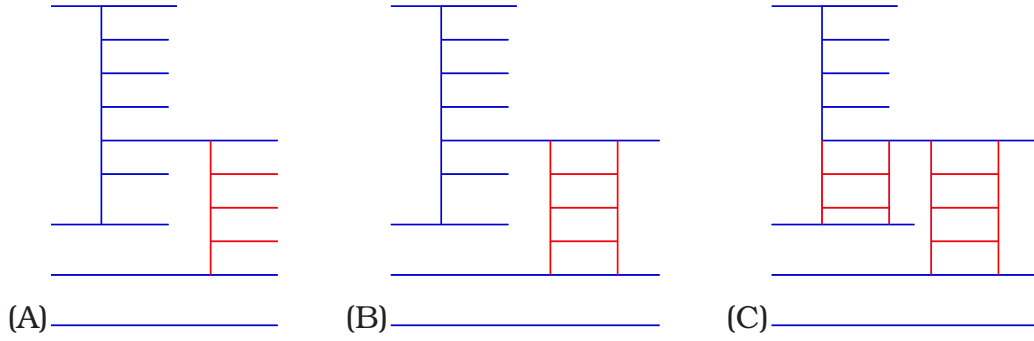


Figure 4: Multiple ladders (left), elastic interacting (middle), rapidity gap events (right).

later.

So we try to put all this together

- ☐ In a simple and transparent way
- ☐ using just simple ladders between projectile and target (Pomerons)
- ☐ putting all complications into “projectile / target excitations”, to be treated in an effective way

as shown in figs. 5, 6, 7. Bifurcation of parton ladders will not be treated explicitly, they are absorbed into target and projectile excitations, visualized as fat lines in the figures. The excitations may represent one, two, or even more ladders, depending on the parton densities.

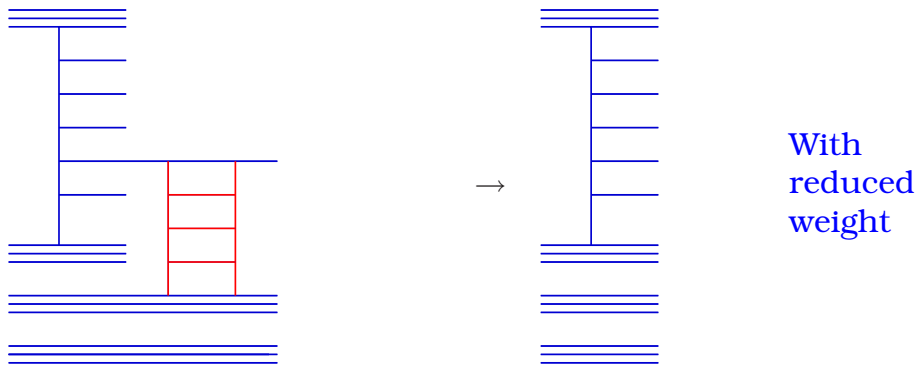


Figure 5: Screening contribution: treated as simple parton scattering, but with reduced weight, to be referred to as screening correction.

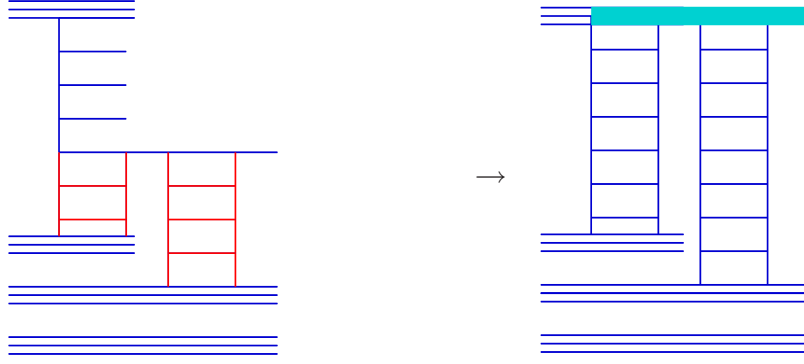


Figure 6: The diffractive contribution: The fat line represents a projectile excitation.

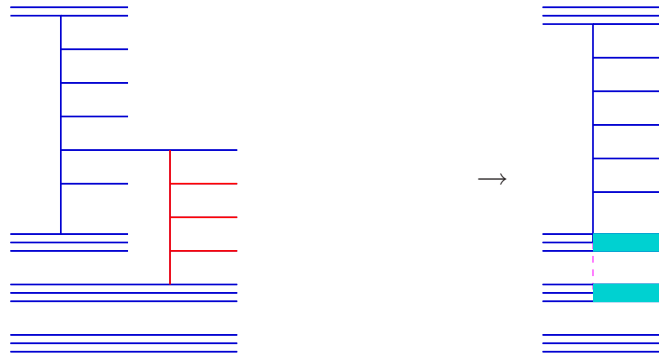


Figure 7: Multiple ladder contribution: A target excitation may represent several ladders.

How to realize the screening correction?

A simple diagram is roughly given as $(x^+)^{\beta}(x^-)^{\beta'}$, and adding the screening diagram will reduce the contribution, which we realize via $(x^+)^{\beta}(x^-)^{\beta'+\varepsilon}$ with some positive parameter ε , which suppresses small x . ε should increase with the number Z of “close” partons, so ε should be a monotonically increasing function of Z . What are close partons? Their number Z should increase with decreasing b and it should increase with energy. We use

$$Z_{P/T} = \sum_{\text{nucleons}} \frac{E}{E_0} g\left(\frac{b}{b_0}\right)$$

with

$$g(x) = \frac{1}{\sqrt{a^2 + x^2}} \exp(-x^2),$$

and

$$\varepsilon = \varepsilon_{\max} \left(1 - \frac{1}{\sqrt{1 - (\log(1 + 3Z))^2}} \right)$$

How to realize projectile / target excitations ? (accounting for multiple, interacting (?) ladders)

- ☐ We suppose an excitation mass distributed according to $1/M^{2\alpha}$.
- ☐ For masses exceeding hadron masses we take strings.
- ☐ String properties are supposed to depend on Z

(the string represents multiple, interacting (?) ladders)

For the moment we take $\langle p_t \rangle_{\text{break}} = \langle p_t \rangle_{\text{break}}^0 f(Z)$ with $f(Z) = \min(f_{\text{max}}, 1 + \alpha Z)$, $f_{\text{max}} = 3$, $\alpha = 0.3$, which gives $Z \lesssim 2$ for pp, $Z \lesssim 6$ for d-Au.

The formalism is based on cut diagram techniques, strict energy conservation, and Markov chains for the numerics [3].

3 Some results

In fig.8 we show the different contributions to the pseudo-rapidity distribution in pp collisions, compared to data from [4], and a transverse momentum distribution of charged particles (data from [2]).

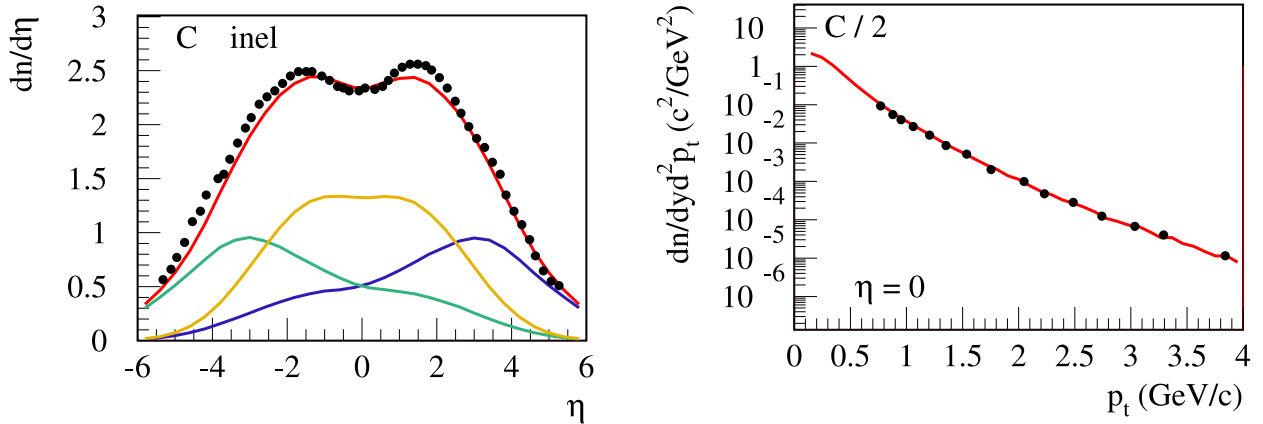


Figure 8: Left: The different contributions (central ladders, target excitations, projectile excitations) to the pseudo-rapidity distribution. Right: Transverse momentum distribution.

Let us turn to d-Au scattering. At this point there is no fine-tuning employed. We first want to understand the qualitative features of our effective treatment of

interacting parton ladders (projectile / target excitations). In figs. 9, 10 we show the centrality and the pseudo-rapidity dependence of the nuclear modification factor, showing clearly the effect of an increased transverse momentum due to interacting ladders.

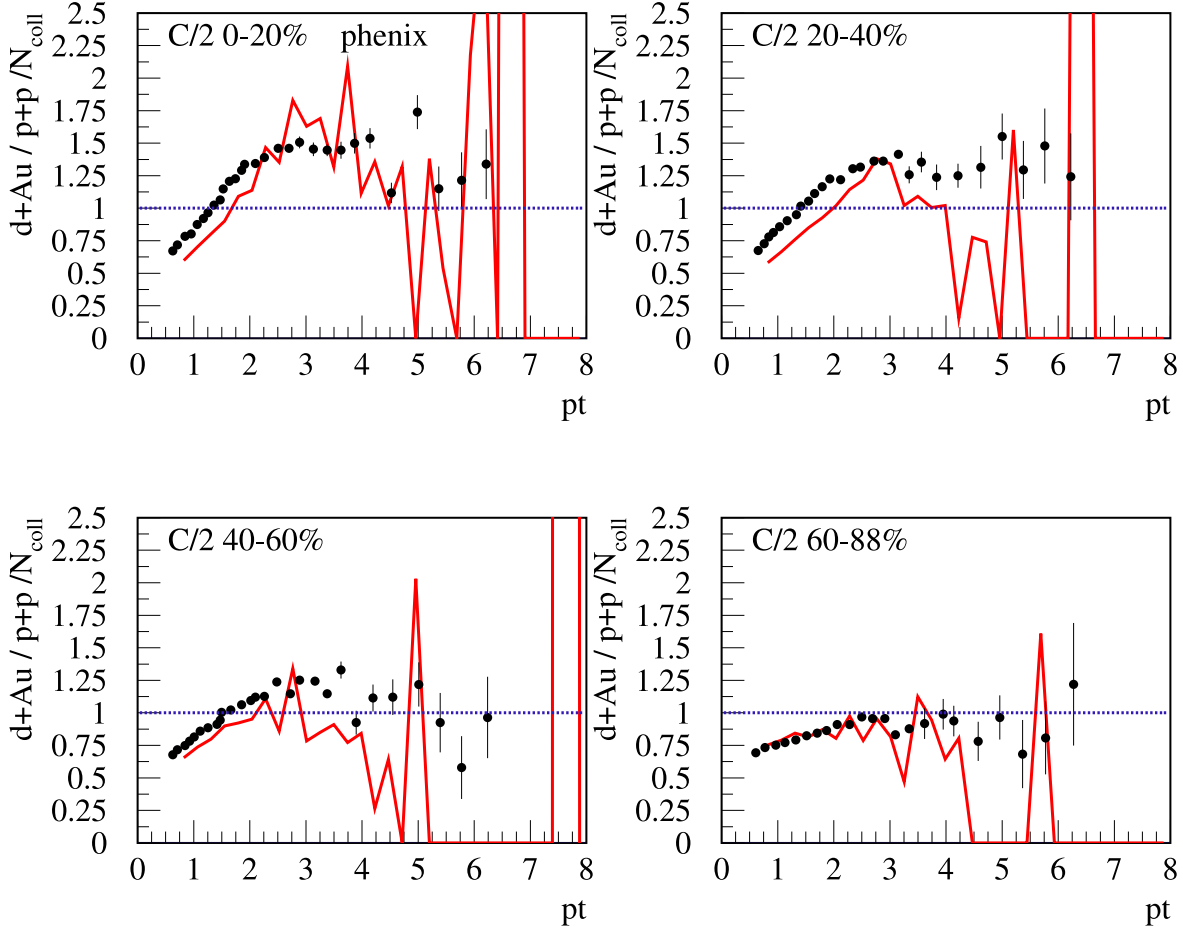


Figure 9: Centrality dependence of the nuclear modification factor.

References

- [1] Phenix collaboration, Phys. Rev. Lett. 91:072303 (2003)
- [2] Brahms collaboration, nucl-ex/0403005
- [3] H.J. Drescher, M. Hladik, S. Ostapchenko, T. Pierog, K. Werner, Phys. Rept. **350** (2001) 93
- [4] The Phobos collaboration, Phys. Rev. Lett. 91:072302 (2003)

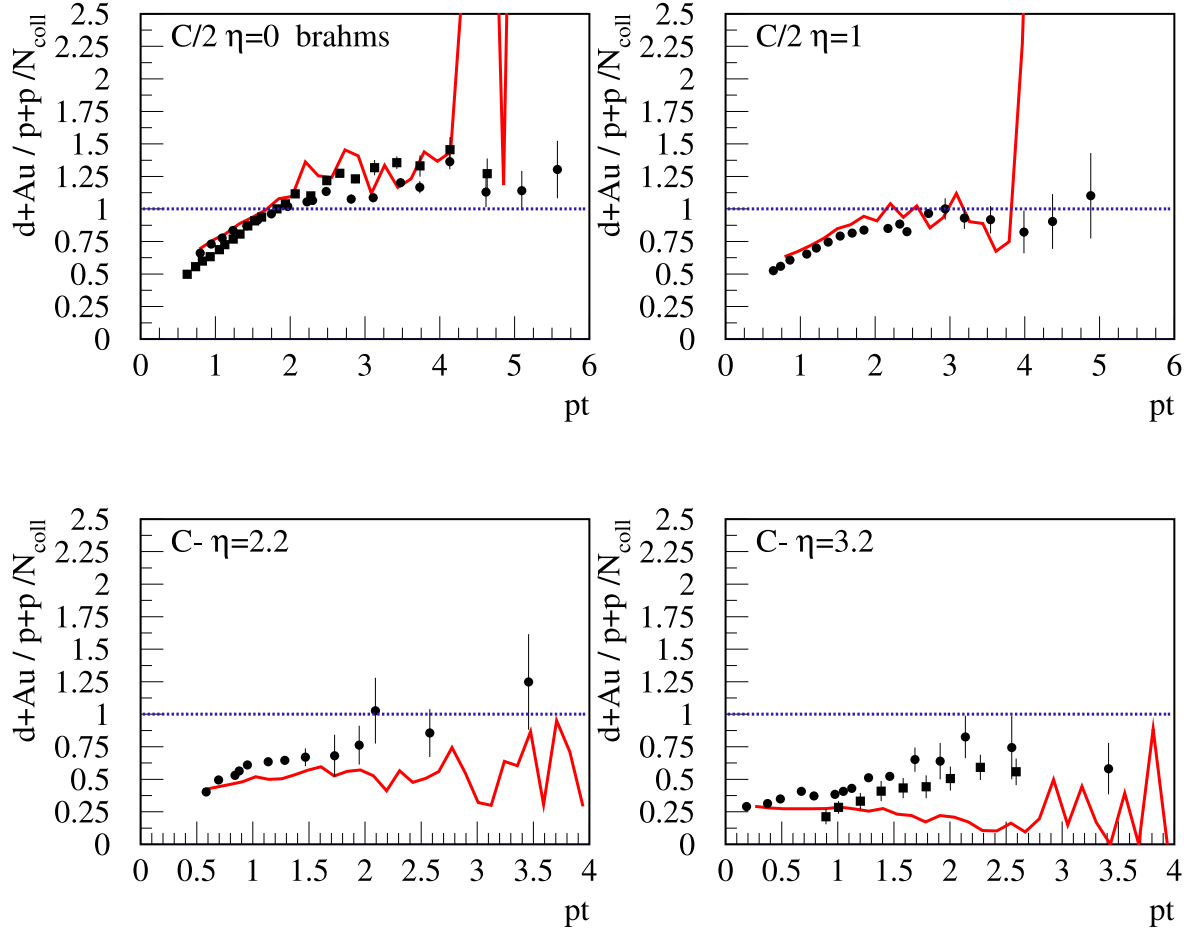


Figure 10: Pseudo-rapidity dependence of the nuclear modification factor.